A Hail Climatology of the Netherlands

Wouters, Lucas; Boon, Maaike; van Putten, Demi; van 't Veen, Bram; Koks, Elco; de Moel, Hans

2019

citation for published version (APA)
Wouters, L., Boon, M., van Putten, D., van 't Veen, B., Koks, E., & de Moel, H. (2019). *A Hail Climatology of the Netherlands*.

IVM Institute for Environmental Studies

A hail climatology of the Netherlands

Wouters L.A., Boon M., van Putten D., van t' Veen B., Koks E.E. & de Moel H.

Climate-KIC

24 December 2019

Contents

Summary

Convective storms that produce large hail are among the most damaging natural hazards and globally losses due to these events are increasing. To evaluate and quantify the potential risk associated with these storms, hail climatologies are created from historical records. Unfortunately, a comprehensive analysis of the Netherlands does not exist.

The aim of this study is to create a hail climatology of the Netherlands and report on spatial and temporal hail risk by combining two approaches. The first approach relies on written documents containing information on historic events collected from *Weerspiegel*-magazine and the *European Severe Weather Database* (ESWD), from the time period 1974-2019. The second approach utilizes radar-data from the time period 2008-2019 and implements a radar-based Hail Detection Algorithm (HDA) to estimate hailstone sizes.

From a total of 7559 report-based observations in the time period 1974 -2019, it is found that 81% of severe hail events are observed in the months from May to August with the majority (53%) reported between 14:00 and 19:00 local time. The return period estimation from the observed hail sizes indicates an occurrence of 1 in 100 years in the case of diameter equal or larger than 11 cm and 1 in 10 years of diameter equal or larger than 7 cm for the Netherlands. It is found that the Northern NUTS region of the Netherlands is 3.5 times less likely to experience a hailstone of 6 cm than the Southern NUTS region. The radar-derived hail observations show an increasing gradient in the number of (severe) hail days going from the Northwest to the Southeast. Additionally, the latter region shows the highest averaged values of Maximum Estimated Size of Hail (MESH). By clustering hail events into individual storms, an increasing trend in MESH values was observed with increasing hailstorm extent, though large hailstone sizes can also occur in small hail streaks.

To further extend knowledge on this topic, it is recommended to conduct quantitative research on the effect of climate change on the formation of severe hail and possibly apply synthetic data to generate longer records. Moreover, recommendations are made to improve short-term measures against hail damage by developing nowcast systems and potentially combining these with real-time information from social media.

1   Introduction

Severe hail events have the potential to impact society by producing significant damage to people, crops and property. Worldwide, the increasing trend in losses due to convective storms asks for a better understanding of the temporal and spatial characteristics of related risks (Munich RE, 2019). The relevance for updated hail knowledge in the Netherlands was demonstrated by the events of the 23rd of June 2016. During this storm, hailstones up to 10 cm in diameter caused over 500 million in damage to roofs, vehicles, agriculture, greenhouses and solar panels (Verbond Van Verzekeraars, 2017).

This study is part of the EIT Climate-KIC program: '1-million near-zero energy (NZE) homes in 2023'. The EIT Climate-KIC is a European public-private partnership focused to tackle climate change and building resilient, net zero-carbon societies to limit global warming to 1.5ºC in 2050 (EIT Climate-KIC, 2018). Several measures to houses can be taken to reach this goal, such as solar panels and external wall insulation. However, the transition towards a carbon-neutral society may be hampered by the impacts of extreme weather damaging these NZE measures. To mitigate the damage of future events, it is desirable to provide stakeholders with a more thorough understanding of the risks associated with severe weather events. Hail climatologies layout records of past events and can be used to evaluate and quantify hail risks, including the frequency, intensity and characteristics. Currently, several countries affected by severe hail events have established these climatologies based on quantitative information provided by meteorological observatories (Cintineo, et al., 2012), eye-witness reports (Groenemeijer & van Delden, 2005) or hailpad networks (Fraile, et al., 2003) (Burcea, 2016). Unfortunately, the absence of reliable and consistent data collection has hampered a comprehensive analysis of the Netherlands.

Although preliminary research was conducted based on historical witnesses by (Groenemeijer & van Delden, 2005), the lack of homogeneity of these reports means that the spatial distribution from written sources could be biased. With the emergence of modern remote sensing instruments and dual-polarization radar, proxies of hail size can be created which are not restricted to inhabited areas or biased by the availability of potential observers (Punge & Kunz, 2016). However, validation of these proxies remains difficult due to the inhomogeneous nature of historic hail observations and ground truth reports (Salitkoff, et al., 2010).

Another component of hail severity is the dimensions of the storm in terms of length, width and orientation. The spatial extent of an area affected by hail is called a hail streak and (Punge & Kunz, 2016) show that the average size of such a hail streak varies greatly per location. In central Europe, it is usually smaller than 500 km2, but in the U.S. hail streaks often affect areas of even less than 40 km^2 with an average of 20.5 km^2 . However, the study also mentions little is known on the regional variations of the extents of large hailstorms and the relation to severity. Therefore, this study will link the extent of hailstorms in the Netherlands to maximum estimated hail sizes.

This study reports on the development of a hail climatology for the Netherlands through the examination of documented written sources and the implementation of a radar-based Hail Detection Algorithm (HDA). From this climatology, the probability of certain hailstone sizes will be derived, as well as spatial differences in the Netherlands and the size of hailstorm events. Overall, the climatology and associated hail hazard characteristics provide crucial information for planning and managing hail risks by a variety of actors (e.g. farmers, property owners, insurers, etc.). Moreover, it supports

the development of a now-casting system, which can be used for short-term forecasting and informing the public of hailstorms coming their way, enabling damage-reducing measures and behavior.

1.1   Report outline

This report is divided into four chapters. In the first chapter, the theoretical dimensions regarding local and global hailstorms are provided. The second chapter focusses on the available data, preparation and the implemented methodology. In the third chapter, the results of the various temporal and spatial climatology products are presented and assessed with respect to the objective of this study. It will then go on to chapter 4 to discuss the results in context to other climatologies, the effect of climate change, synthetic event-based datasets and current state of research on nowcasting systems. The final chapter concludes the report by summarizing its main results, limitations and recommendations for future assessments.

2   Background information

This chapter describes the relevant background information related to hail in general, and in the Netherlands in particular, including its characteristics.

2.1   Severe hail formation

Hail is formed in thunderstorms with strong vertical air motions due to thermodynamic instability. The convective updrafts displace moisture above the freezing level to form supercooled water droplets that condense on a surface, such as dust, to form hailstones (Allen, 2017). The hailstones keep growing by the accretion of additional liquid water and collisions between individual hailstones (Mahoney, et al., 2012). Once the hailstones are no longer supported by surrounding rising air motions due to their size and weight, they begin to fall. Hail formation is typically tied to more intense and long-lived thunderstorms with stronger updrafts and increased wind shear (Allen, 2017).

Several convective parameters are linked to the formation of hail, the intensity of the storm, and hail sizes. Convective available potential energy (CAPE) refers to the positive temperature difference between an idealized parcel of air and its surroundings (Riemann-Campe, Fraedrich, & Lunkeit, 2009). A larger value for CAPE, therefore, indicates a stronger convective updraft. The counterpart to CAPE is convective inhibition (CIN). CIN is the intensity of the stable layer in the atmosphere an air parcel needs to overcome in order to develop convection. CIN is, therefore, able to inhibit convection while very high values of CAPE exist (Riemann-Campe, et al., 2008). Another convective parameter is the lifted index (LI), which is defined as the difference between the observed temperature and the air parcel after it has been lifted from its original level to 500hPa and is a measure of stability of the atmosphere (Vujović , et al., 2015). The lower the values for LI, the higher the chance of thunderstorms to develop with heightened risk for severe weather. Moreover, the sea effect contributes to the inhibition of large hail by lower temperatures in Northern Europe. Although the influx of moist air leads to frequent showers of graupel and small hail, extreme instability is suppressed by cooler air flows. For the Netherlands, convective activity is strongly influenced by the North Atlantic Ocean (Punge & Kunz, 2016).

Although some variation is found, it is commonly accepted that severe hail is defined by the hail diameter. In this research, severe hail is defined as hail with diameters of 2 cm. At this point, hail damage becomes substantial to most crops, with the probability of hail damage to roofs, windows and vehicles increasing strongly as hail size exceeds 5 cm (Púč ik, et al., 2019). The research of (Teule, et al., 2019) shows that houses and solar panels also are at risk of being damaged by hailstones of 2 cm.

2.2   Hail response to climate change

It is largely unclear what effect a warming climate has on the frequency and intensity of hailstorms (Mahoney, et al., 2012). New research suggests a decrease in days with small hailstones due to a higher melting level which results in a decreased proportion of precipitation reaching the surface as hail versus rain (Mahoney, et al., 2012; Allen, 2017). On the other hand, both the mean hail size and frequency of larger hail events have the potential to increase, as was found for research conducted in North America (Allen, 2017). Both results have been found in multiple studies concerning hailstorm frequency and intensity in various locations across the globe (Mahoney, et al., 2012;

Brimelow, et al., 2017; Zou, et al., 2018). These seemingly opposing results can be ascribed to the physical processes related to hail formation.

Smaller particles melt more quickly than larger ones, and at levels nearer to the melting level. Due to projected increasing atmospheric temperatures, the height of the melting level increases, resulting in the earlier onset of hailstone melt. Contrarily, a climate with higher temperatures and more atmospheric moisture produces thunderstorms with stronger updrafts, resulting in increased hail production (Mahoney, et al., 2012).

Dennis and Kumjian (2016) found that increased deep-layer east-west shear elongates the updraft in that direction, providing three circumstances that lead to increased hail mass: (1) a larger volume over which micro-physically relevant hail processes can act, (2) increased residence times of hailstones within the updraft, and (3) a larger region for new hailstones to form.

Ilotoviz et al., (2015) found that a change in atmospheric aerosol concentrations leads to a change in the major mechanisms of hail formation and growth. The main effect of increased aerosol concentration was found to be an increase in the supercooled cloud water content. Therefore, at high aerosol concentration, hail grows largely by accretion of cloud droplets in the cloud updraft zone. In the case of low aerosol concentration, freezing of raindrops is the main mechanism of hail formation (Ilotiviz et al., 2015).

2.3   Challenges in determining trends in hailstorms

Storms usually develop at small spatial and temporal scales. Hermida et al., (2013) found high variability in spatial, altitudinal and temporal trends with opposing results between very close network stations because of the small scale of the hailstorms. The main issue can be ascribed to the scarcity and poor standardization of hail detection and monitoring systems (Sanchez, et al, 2017).

For Europe, specific spatial trends for hail could not be identified due to the lack of hail monitoring and data gaps. For individual stations, trends for convective parameters describing latent instability such as CAPE and LI are available which can be linked to the potential hail response. The surface-based CAPE and LI show increasing trends for Europe between 1978 and 2009, relating to a higher convective potential (Mohr & Kunz, 2013). For global trends, CAPE is shown to follow the distribution of near-surface temperature and specific humidity, with CAPE values generally increasing from pole to equator. Higher values for CAPE are generally found in the summer northern hemisphere (June, July, August) and in the summer southern hemisphere (December, January, February) (Riemann-Campe, et al., 2008). Spatial trends for CAPE and CIN are variable and do not show specific global patterns. However, globally CAPE shows increasing trends from 1958 – 2001 during all seasons, whereas CIN shows a general increase from December to August and a decrease during September, October and November. This would result in a higher chance of storm genesis during autumn when CAPE is high and CIN is low (Riemann-Campe, et al., 2008).

3   Data and Method

This section will describe available data and the methodology implemented in this study. In the first section, the available data are discussed. The second section will focus on the applied method.

3.1   Data

3.1.1   Observed hail sizes

Hailstone sizes have been extracted from eye-witness reports in the monthly magazine *Weerspiegel* and *the European Severe Weather Database* (ESWD) to create an observed-hail dataset. This dataset includes the date and location of observed hailstorms, and, when mentioned, the time of occurrence or time frame, range of observed hail sizes (cm), maximum observed diameter (cm), wind gust speed (m/s), other forms of precipitation and additional notes.

Weerspiegel magazine is established by meteorologists and overall weather enthusiasts in the Netherlands. All editions in a time period of 1974 to 2019 have been examined manually to provide this study with the written sources of hailstorm events. In this magazine, observers report on the date and general location of events, occasionally including the diameter of the hailstones and the exact time of the observation. Next to this information, an indication of the number of lightning strikes, other forms of precipitation and additional wind gust speed (if ≥ 13.9 m/s) are given. The total amount of entries from *Weerspiegel* is shown in table 1.

Additionally, the ESWD, operated by the *European Severe Storms Laboratory* (ESSL), was consulted to augment the dataset. This database contains reports on severe convective storm events over Europe. Reports in this database include the coordinates of the observed storm and in most cases also its time frame and storm duration. The ESWD also reports on *Weerspiegel* observations in several instances. In that case, duplicates are removed from the dataset. The total amount of entries from the ESWD is shown in table 1.

Table 1. The total amount of observations included in the observed-hail dataset from Weerspiegel-magazine and the ESWD.

Source	Total observations	# of hail sizes	# of hail sizes ≥ 2 cm
Weerspiegel	7.393	503	173
ESWD	166	150	148

3.1.2   Radar data

The KNMI currently utilizes two active C-band Doppler radars from the Meteor 360 AC type, with towers in Herwijnen (51.8369 NB, 5.1381 OL) and Den Helder (52.9533 NB, 4.7900 OL). These radars transmit energetic pulses with a peak power of 250 kW with the receiver of the radar measuring the reflected signal into a measure of reflectivity and particles per unit volume. The radars use 4.2 m diameter parabolic antennas offering a 1-degree beam. Radar composites are available with a temporal resolution of 5 minutes

and a spatial resolution of 1 km^2 , covering the whole of the Netherlands (Holleman, 2001).

3.1.3   Model data

The KNMI operates the High-Resolution Limited Area Model (HiRLAM), from which meteorological parameters such as surface pressure, atmospheric temperature, wind, and humidity can be retrieved. HiRLAM is a hydrostatic gridpoint model that covers a part of the total atmosphere and uses lateral boundary values from the global model of the European Centre for Medium-range Weather Forecasts (ECMWF). The D11 version of HiRLAM was used to calculate environmental temperature levels, also referred to as isotherm heights, using the geopotential and temperature at 60 vertical model levels. HiRLAM D11 runs are available in a temporal resolution of 3 hours and a spatial resolution of 0.1° x 0.1°.

3.2   Method

The method compromises of 3 main sections. The first section covers the chosen approach to estimate return periods from certain hail stone magnitudes. In the second section, a method is presented to create hail size proxies through using radar reflectivity in combination with data from numerical weather prediction (NWP) models. The last section describes the approach of determining the spatial extent of an area affected by hail and its relation to the maximum estimated hailstone size (MESH).

3.2.1   Return period estimation

To give an approximation of the probability of events with a certain intensity, return periods are created based on reports from the hail dataset. A return period, commonly measured in years, is statistically derived from historical data and widely used in extreme value and risk analysis to provide the probability of exceedance of events with a magnitude greater than a certain level (i.e. a return period of once in 20 years for hailstones with a size of 8 cm means that every year there is a 5% chance of hailstones of 8 cm or higher occurring).

In general, two approaches to extreme value analysis can be applied. The first approach looks at the distribution of block maxima (with a block being a defined time period, often a year) and the second approach, the Peak Over Threshold (POT) looks at all values that exceed a predetermined threshold.

The block maxima approach consists of selecting the maximum observations from non-overlapping time periods that are equal in size. In this study, the highest value in each calendar year was selected to represent an independent block of the time series. Therefore, the block maxima approach will from now on be referred to as Annual Maxima (AM). The chosen distribution to fit the data is the Generalized Extreme Value (GEV) distribution, with the Cumulative Density Function (CDF) given by:

for extreme value z,

$$G(z) = \exp[-\left\{1 + \xi \left(\frac{z - \mu}{\sigma}\right)\right\}]_+^{-1/\xi}$$

Where σ is a multiplier that scales function, ξ is the parameter that describes the relative distribution of the probabilities and μ the position of the GEV mean. The resulting return level (z_p) is interpreted as follows:

$$G(z_p) = 1 - p$$

where z_p is expected to be exceeded on average once every $1/p$ period.

A drawback of this approach is that a relatively small subset of the data is taken to represent the extreme events. To use the dataset more efficiently, a POT-method is proposed. The POT-method considers all events that have an independent exceedance over a predetermined threshold value. The chosen distribution to fit the data is the Generalized Pareto (GPA) distribution, with the CDF given by:

for threshold excess x,

$$H(x) = 1 - [1 + \xi \left\{ 1 + \xi \left(\frac{x - u}{\sigma_u} \right) \right\}]_{+}^{-1/\xi}$$

where u is the reference value for which GPA excesses are calculated. The resulting return level (x_m) is interpreted as follows:

$$x_m = u + \frac{\sigma_u}{\xi} \left[(m\zeta_u)^{\xi} - 1 \right] \qquad \xi \neq 0$$

$$x_m = u + \sigma_u \, ln(m\zeta_u) \qquad \xi = 0$$

where x_m is exceeded every m times and ζ_u is the probability of exceeding the threshold.

The application of the POT-method requires the determination of a threshold that includes enough observations for the analysis while excluding values that are not considered extreme. In literature, there is no clear consensus in the best estimation of the threshold value and often is referred to previous studies or engineering judgement (Bezak, et al., 2014). For this study, a threshold value of 2 cm is chosen, as this corresponds to the size at which hail is usually considered severe.

3.2.2   HDA

In this study, the HDA as suggested by (Witt, et al., 1998) is used to compute MESH values, which refers to the hailstone diameter (mm). The MESH parameter is empirically derived from the Severe Hail index (SHI), which is a thermally weighted vertical integration of the reflectivity from the melting level to the top of the storm.

The first step is to calculate the hail kinetic energy ($\dot{E}$) related to reflectivity as adapted from (Waldvogel, et al., 1978):

$$\dot{E} = 5 \times 10^{-6} \times 10^{0.084Z} W(Z)$$

where Z is the horizontal reflectivity factor in dBZ and $\dot{E}$ is in $J \, m^{-2} s^{-1}$. In this formula, a reflectivity weighting function is applied. By not considering reflectivity lower than 40 dBz, values often associated with liquid water are filtered out. The weighting function is given by:

$$W(Z) = \begin{cases} 0 & for \, Z \leq Z_L \\ \dfrac{Z - Z_L}{Z_U - Z_L} & for \, Z_L < Z < Z_U \\ 1 & for \, Z \geq Z_U \end{cases}$$

where Z_L and Z_U are 40 dBZ and 50 dBZ, respectively. Values higher than 50 dBz are assigned a weight of 1.

The significant hail index (SHI) is defined by:

$$SHI = 0.1 \int_{H_0}^{H_T} W_T(H)\dot{E}\, dH$$

where H_T is the height of the storm cell and H_0 is the height of the environmental melting level above radar level. Hail is assumed only to occur at subzero conditions and is maximized when the temperature is at or below -20°C. This assumption is represented by the following temperature-based weighting function:

$$W_T(H) = \begin{cases} 0 & for\ H \leq H_0 \\ \dfrac{H - H_0}{H_{m20} - H_0} & for\ H_0 < H < H_{m20} \\ 1 & for\ H \geq H_{m20} \end{cases}$$

where H_{m20} is the height of the -20°C environmental temperature. Both H_0 and H_{m20} are determined using the output of the HiRLAM NWP model.

Given the SHI value, the MESH output is derived with the following formula:

$$MESH = 2.54(SHI)^{0.5}$$

Clutter, or unwanted echoes in radar, could cause misclassification of ground objects as hail. This is mainly a result of the refraction of radar beams due to shifting densities with height. Although this could lead to radar reflects off buildings, wind turbines or other structures, this issue is not addressed as the focus of this study is on regions rather than individual objects or pixels. Clutter is unlikely to produce significant differences that influence the climatology.

3.2.3   Day selection criteria

The main advantage of using radar data as opposed to written sources is its temporal consistency and spatial coverage. However, computing the MESH for all available timeframes of radar data would include irrelevant days and lead to a computationally heavy analysis. Therefore, days with favorable conditions for hail formation are selected based on the values of Convective Available Potential Energy (CAPE) and a sufficiently small Convective Inhibition (CIN). As the occurrence of severe hail formation increases with higher instability, certain selection criteria can be set to select relevant hail days (Groenemeijer & van Delden, 2006). To create a hail climatology in this report, the following thresholds of CAPE and CIN are used:

$$CAPE \geq 1500\ Jkg^{-1}$$
$$CIN \leq -100\ Jkg^{-1}$$

3.2.4   Validation criteria

To evaluate the hail size proxies from the HDA, ground truth values from the hail dataset are used. However, the exact time, as well as the location at which the hailstone is found, is often not reported. Because of the highly localized nature of hailstorms, this deviation in time and space could yield undesirable results.

To adjust for this uncertainty, validation is conducted that considers a time window of 30 minutes around the reported time and a radius of 3 km and 5 km around the reported coordinates.

3.2.5   Storm extent

To evaluate the relation between the storm footprint and the MESH corresponding to this footprint, an approximation of the 'true' extent of an event was made. This extent was determined by applying a clustering of all daily maximum MESH values from the HDA output.

Clustering was performed by Queen Contiguity, meaning that neighbouring features either connecting a corner or an edge were assigned the same cluster-id (Dubin, 2009). All non-zero features in the data (pixels with values) were features. Zero features (pixels without value) are background and therefore not evaluated in the analysis. For each cluster id, the corresponding MESH was extracted. A visualization of the clustering process is shown in figure 1. As the scope of this study is on the Netherlands, the radar output will be clipped to fit the extent of the Dutch border.

To evaluate the relationship between MESH and hailstreak, a threshold for cluster size was applied. Small clusters could exaggerate the relationship or also consider clusters of the same storm. Therefore, all clusters with an extent smaller than 225 km^2 (corresponding to a 15x15 grid) were not included in this analysis.
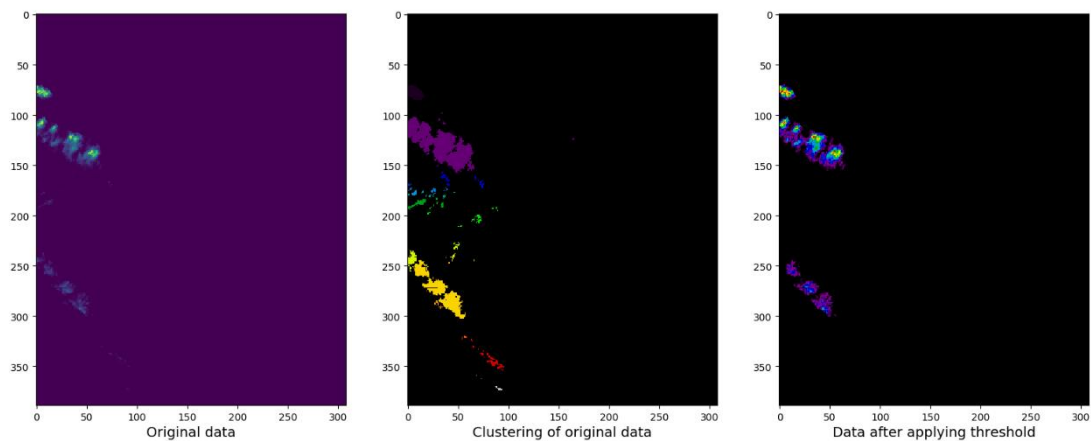

Figure 1. The clustering process of a radar-derived storm extent. The number of unique clusters may be illustrated by the number of different colours in the middle screen in the figure

4   Results

This chapter presents the results obtained from the approaches described in chapter 3. Section 4.1 describes the analysis of the report-based hail dataset. The return period estimation for the Netherlands and its regions is presented in section 4.2. The radar-derived hail maps created for the period 2008 – 2019 are illustrated in section 4.3 together with validation of the hail size proxies computed by the HDA and the report-based observations. In section 4.4 the storm footprint of daily hail composites is related to the corresponding highest value of MESH.

4.1   Documented sources

The monthly and hourly distribution of reported hail events and sizes are illustrated in figure 2 and figure 3, respectively. Events with large hail sizes (≥ 4cm) are observed throughout the year, with peak activity from May to August. In total, 81% of all hail events above 2 cm and 95% of all events with hail larger than 4 cm are reported in this period.

In total 7 observations of hail sizes greater than or equal than 8 cm are made, divided over 4 separate hail days. Both the hailstorm of the 17th of July 1974 in Flevoland and the 14th of May 1985 in Limburg yielded hailstones of 8 cm. On the 23rd of July 2016, hailstones with a diameter of 10 cm were observed in Valkenswaard, Noord-Brabant. On the 6th of June 1998, the largest hailstone ever observed in the Netherlands, with a diameter of 11 cm, was reported Alblasserdam, Zuid-Holland. From all hail reports, most observations are made in Zuid-Holland (1550) and Noord-Holland (1452), and least in Zeeland (254) and Flevoland (100). This distribution corresponds to the total population in Dutch provinces, indicating that population densities could lead to reporting biases.
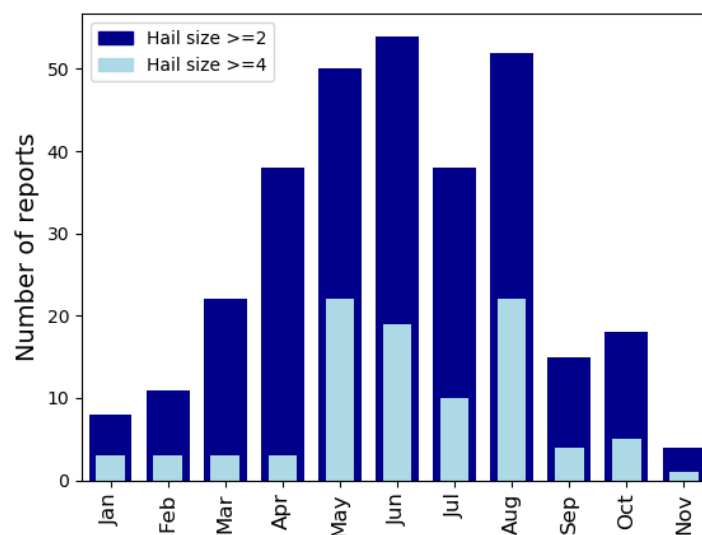

Figure 2. Monthly distribution of reported hail sizes

Figure 3 shows the total amount of reports and their occurrence throughout the day, together with the reports that correspond to the maximum hail size value that day. By doing so, an adjustment is made for the fact that more extreme events also generate more reports. It is observed that the majority of hail occurrence (53%) is reported

between 14:00 and 19:00 local time. The warmest moment of the day is usually reached around 16:00, which indicates the importance of temperature on the updraft and, subsequently, the formation of severe hail. This updraft, caused by strong currents of rising air, carry droplets of water high enough that they freeze and form hailstones.
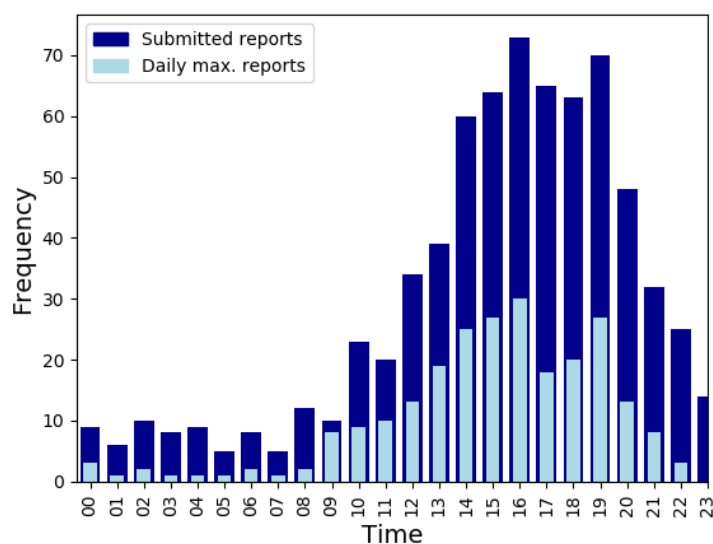

Figure 3. The hourly distribution of the total amount of reported hail-sizes and of the daily max. reports.

4.2   Return periods

Figure 4 gives the extreme value analysis of the Netherlands based on the AM approach. It is observed that hailstones greater than or equal to 7 cm are expected to be exceeded once every 10 years. Based on the GEV distribution, a hail size of 11 cm has a 1%-chance to be exceeded in a year. However, the uncertainty increases with increasing return period because of the limited number of very severe hail sizes.
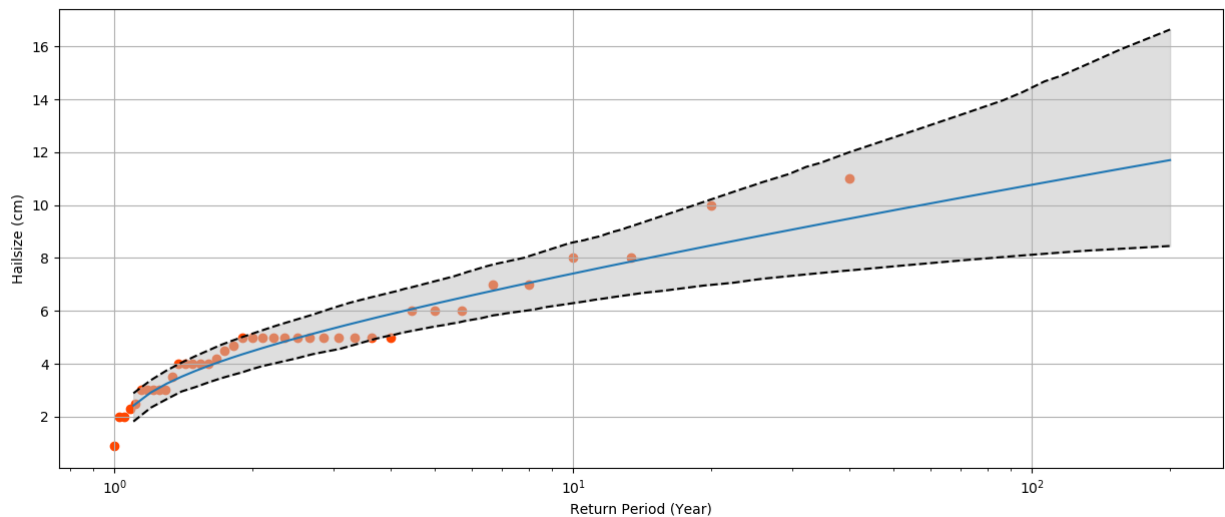

Figure 4. Return period estimation for the Netherlands, based on the GEV distribution and a 95% confidence band.

In figure 6, the observations are divided into the four NUTS1 regions in the Netherlands (North, East, South, West). As the regions resemble each other in surface area, a comparison can be made between them. The results show that the Northern part of the Netherlands is less likely to experience severe hail sizes, with the Southern region yielding the highest exceedance probabilities. For example, it is observed that a 6 cm hailstone corresponds to a 35-year return period in the Northern NUTS region, compared to a 10-year return period in the Southern NUTS region. This implies that the south of the Netherlands has the highest risk of facing hail events, and the north substantially less. For example, the Northern NUTS region is 3.5 times less likely to experience a hailstone of 6 cm than the Southern NUTS region.
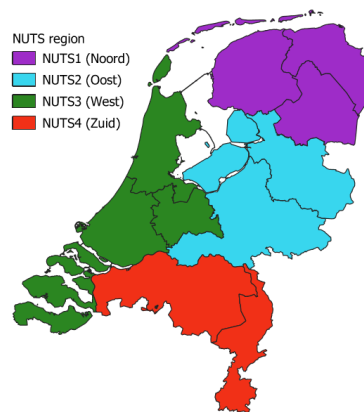
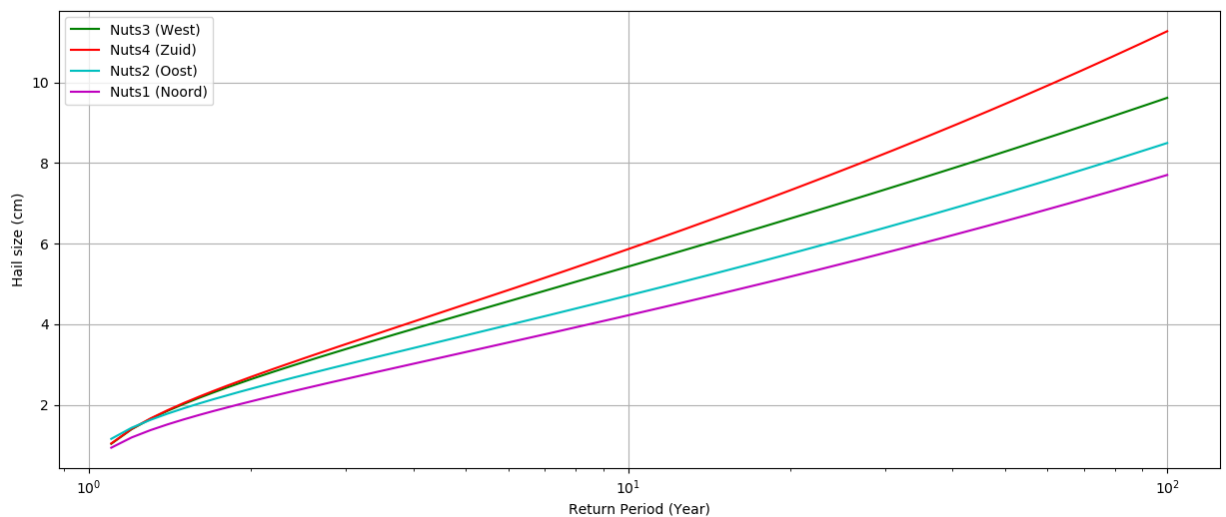*Figure 5. NUTS1 regions in the Netherlands.*

Figure 6. Return period estimation for the 4 NUTS1 regions in the Netherland, based on the GEV distribution.

In figure 7, a comparison between the AM and POT method for extreme value analysis in the Netherlands is shown. Because the POT approach considers all hail values exceeding 2 cm, multiple severe events that occurred in one year are included. The AM considers the maximum annual values of 47 years, where the POT considers 167 values that exceed a threshold of 2 cm. The empirical values and cumulative probability density functions for both approaches converge already from return periods of 3 years onwards, indicating that the different approaches give similar results.
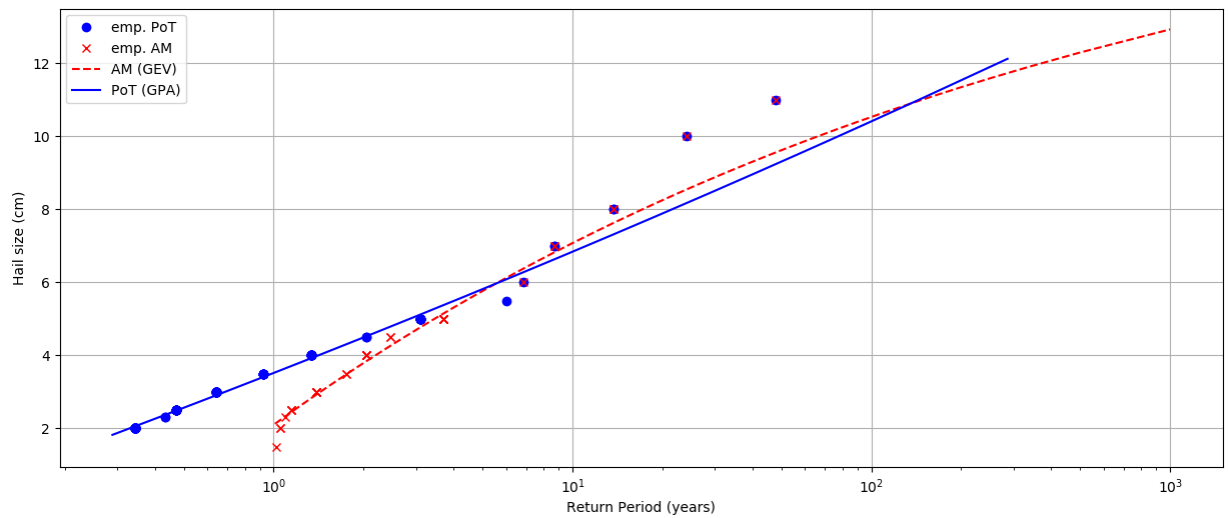
Figure 7. Return period estimation for the Netherlands following both the AM and the POT approach.

4.3   Radar climatology

The spatial distribution of the maximum MESH values for the 11-year time period (2008 -2019) is illustrated in figure 8. Although severe hail values are recorded throughout the country, it shows that the highest concentration of large MESH values is observed in the South-eastern parts of the Netherlands, particularly in Noord-Brabant, Limburg and Gelderland. A total of 328 hail days were selected by the criteria set in chapter 3 and used to create a composite by reducing all MESH values to their maximum recorded value.
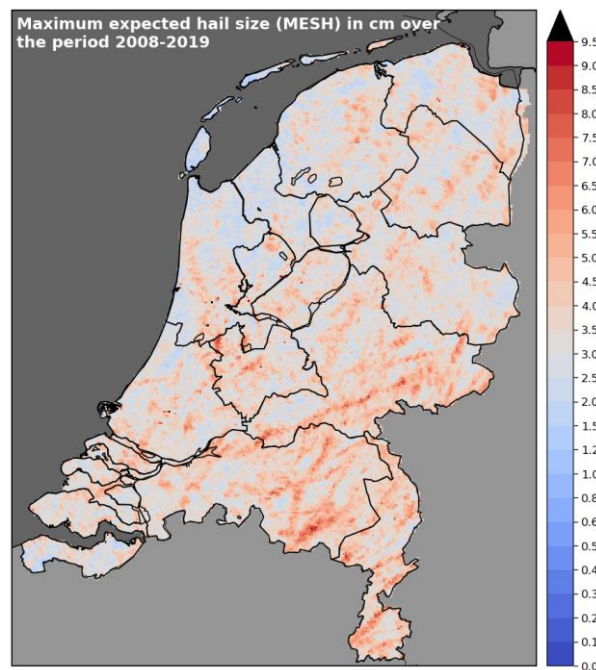
Figure 8. Composite of all max. daily MESH values from 2008 - 2019.

In figure 9, the maximum MESH values of the 23rd of July 2016 hail storm are shown. This figure indicates that individual hail streaks with severe hail sizes have a considerable effect on the resulting hail map in figure 7, in which the same hail streak is clearly visible. In addition, the hail streak follows the same path as the most affected administrative regions (PC4 level) (Teule, et al., 2019). The highest MESH value of this storm day was recorded in Valkenwaard, with a hail size of 9 cm.

Figure 9. A composite of all MESH values computed for the 2016-06-23 hailstorm.

In figure 10, the number of hail days is shown with hail sizes larger than 1 cm and 2 cm. The distribution of severe hail days seems to follow the same trend as figure 7, with incr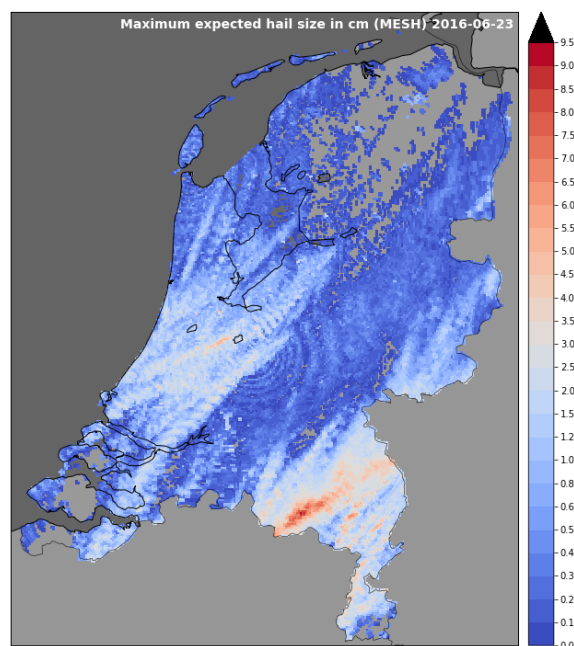easing values towards the South-eastern provinces. The contrast between regions is most clear when considering the number of days with hail larger than 1 cm. This is in line with the return period estimation from *Weerspiegel* and ESWD observations, which also showed this trend. Note however that in the context of this study we consider hail sizes between 1 and 2 cm not severe hail (but sizes ≥ 2 cm).

If observed closely, several individual pixels show an increased number of hail days compared to surrounding pixels. As it is improbable that these 1 km^2 areas experienced considerably more hail than adjacent 1 km^2 areas, these differences are likely to be attributed to ground clutter. This anomaly is found in large cities (e.g. Amsterdam, Rotterdam and Groningen), where buildings could return echoes to the radar, and around harbours (e.g. Eemshaven and Maasvlakte).
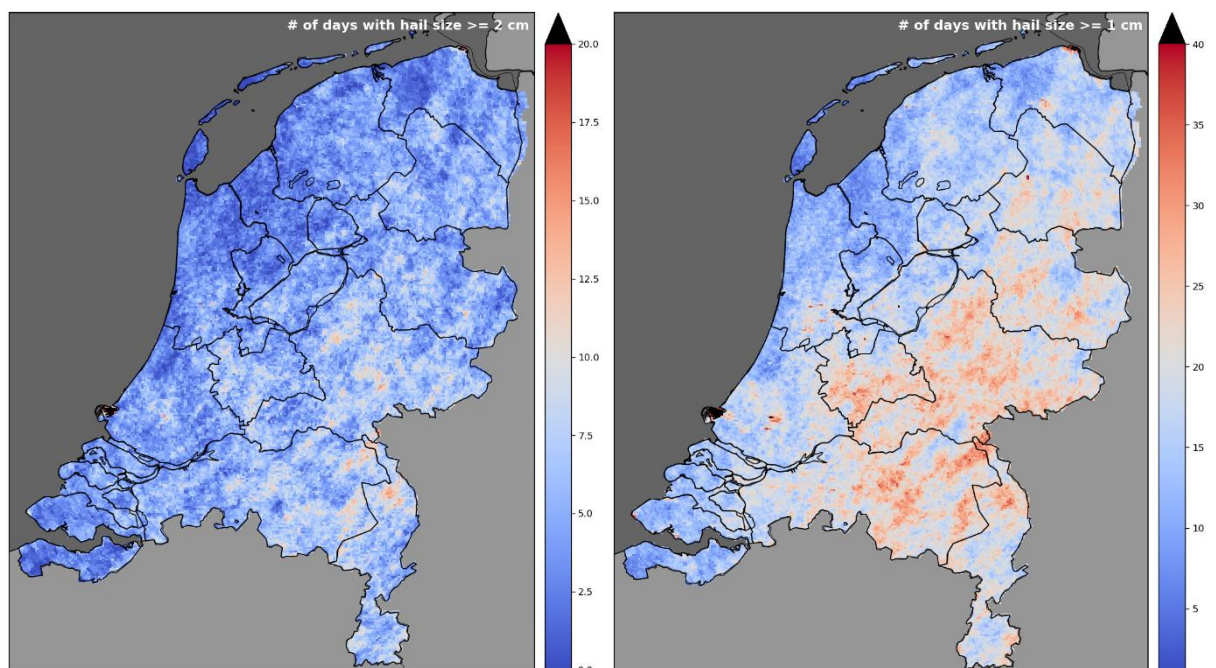
2009. Again, the same trend can be observed with the Southern provinces of Noord-

Figure 10. The number of hail days with hail larger than 1 cm and 2 cm.
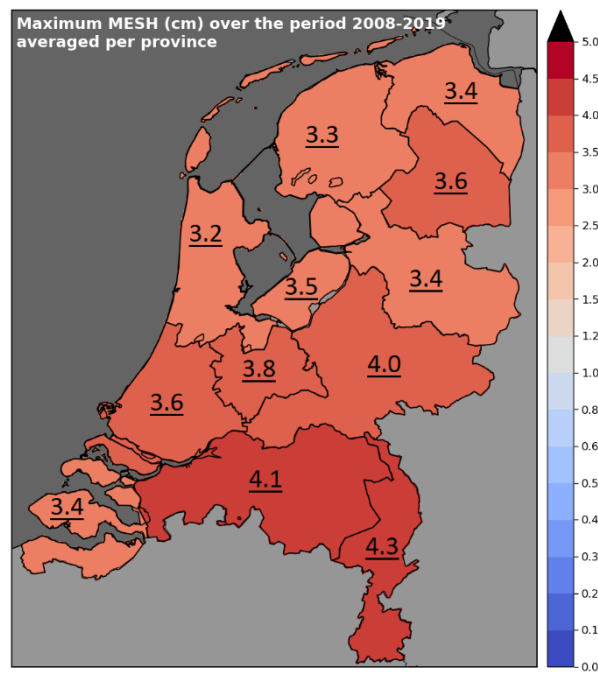
Figure 11. The averaged MESH values per province for the period 2008 - 2019.

4.3.1   Validation of radar products

In figure 12, the relation between the report-based observations and the radar-derived observations is shown. A 1 km radius corresponds to the exact grid location in which the reported hail size is found. The correlation value (R^2) and slope increase by increasing the verification area as observed in table 3.

Hailstone size can be overestimated by the HDA due to the melting of the stone in the air or on the ground. Additionally, the localized nature of hailfall could mean that observers do not necessarily measure the largest stone in the grid area. Underestimation of hail sizes by the HDA is possible due to the radar averaging reflectivity values of the whole resolution volume. If precipitation only accounts for a small part of the radar resolution volume, the measured radar refl ectivity will be lower than the true refl ectivity of the hail present in the limited part of the volume (Bunkers & Smith, 2013). Following this line of thought, it is more likely that hailstones sizes are underestimated in a hailstorm with a large extent.

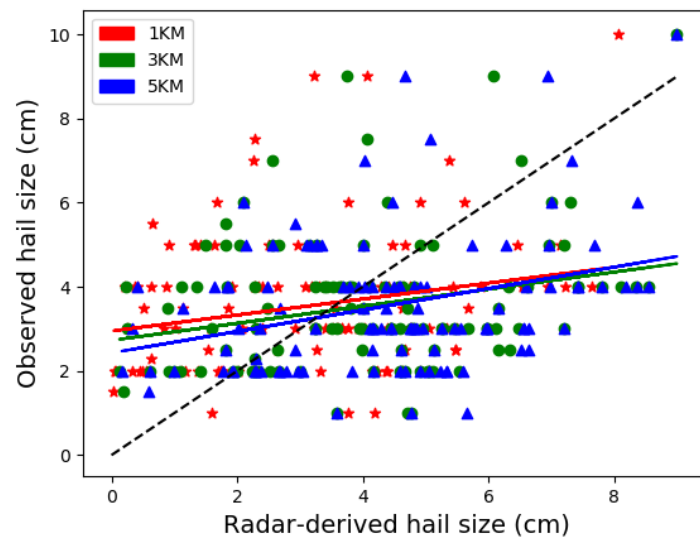*Figure 12. Comparison of the ground truth reports and the modelled hail sizes for multiple radii. The dashed line shows a perfect fit.*

Table 2. The statistical parameters of the comparison between the ground truth reports and the HDA output.

Method	Slope	R^2	P-value
1 km	0.18	0.050	0.016
3 km	0.20	0.065	0.006
5 km	0.26	0.098	0.001

4.4 Storm extent

A total of 41957 storm clusters were identified. After applying a threshold of 225 km^2, 799 unique hail clusters remain for analysis. Descriptive statistics of cluster sizes (e.g. hail streaks) are found in table 4. The extent shows a large variation with a mean of 3495 km^2, a median of 672 km^2 and a standard deviation of 6925 km^2. The corresponding MESH values have a mean of 3.38 cm, with a median of 2.87 cm and a standard deviation of 2.21 cm. The correlation of the storm and its corresponding highest MESH value (figure 13) shows an increasing trend, which means that hailstorms that produce larger hailstones are expected to cover a larger extent of the Netherlands as well. Several MESH values larger than 10 cm and even 15 cm are observed, which could be the result of ground clutter. Ordinary Least Squares (OLS) regression gives a R^2 of 0.231.

Table 4. General storm extent statistics

	Mean	Median	Std. dev
Extent (km^2)	3495	672	6925
MESH (cm)	3.38	2.87	2.21
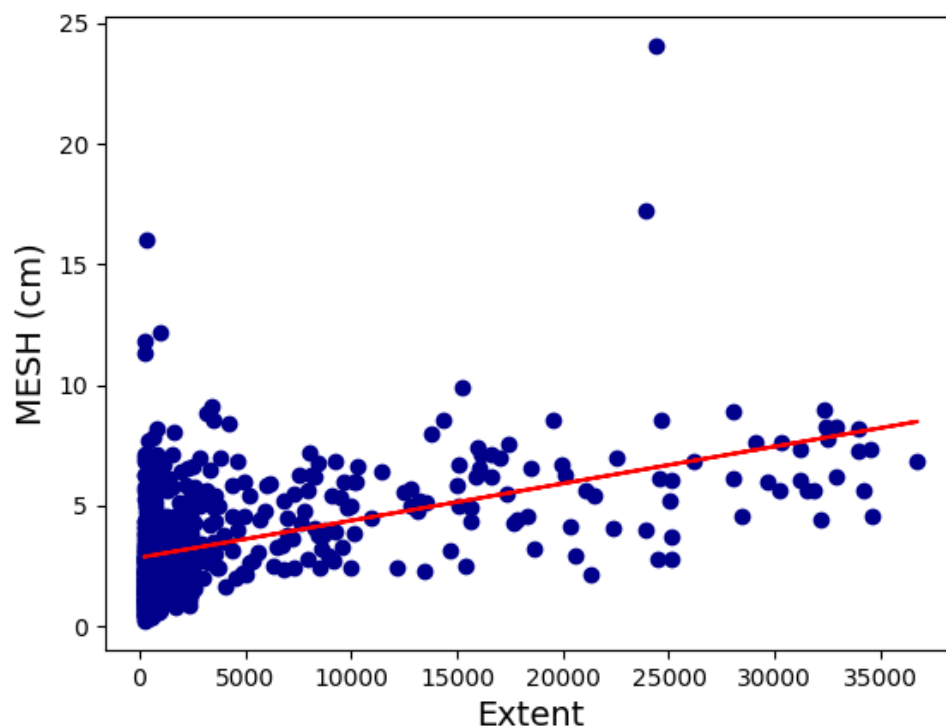
Figure 11. Regression of the MESH and the extent of the corresponding storm.

In figure 14, the frequency of hailstorms with a certain hailstreak is observed. Most hailstorms (61.6%) in the time period of 2008-2019 affected an area smaller than 1000

km^2 . 86.6% of the hail streaks had a footprint up until 8000 km^2. Only 1.5% of the clusters showed extent larger than 32000 km^2.
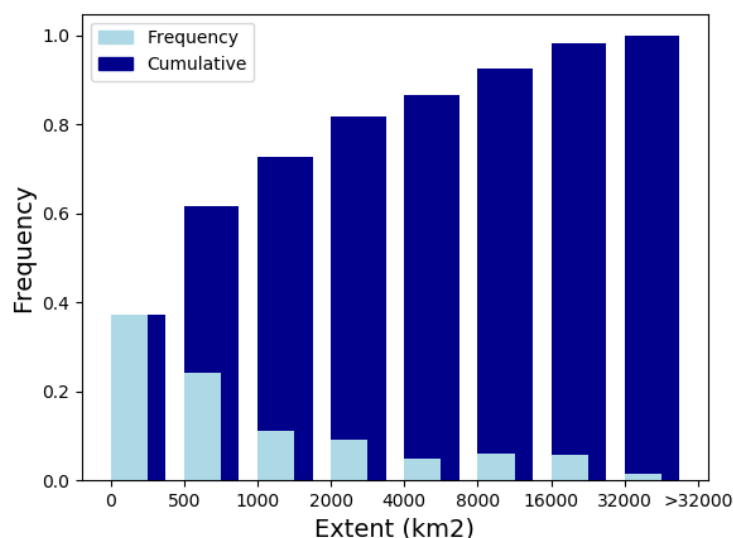
Figure 12. The (cumulative) frequency of the radar-derived storm extents.

In figure 15, the frequency of storms with a certain extent is shown and related to the occurrence of large hailstones. It is observed that in all storms larger than 8000 km^2 , hailstone sizes are greater than 4 cm. Hailstones with diameters over 4 centimeters are nonetheless also present within the smallest extent category. In 12.4% of the smallest extents, MESH ≥ 4 cm was observed. Severe hail occurs in at least 52.2% of all hail streaks.

Figure 13. The frequency of extents corresponding with severe hail values of 2 and 4 cm.

Table 5 describes the statistics for hail sizes (MESH) and their hail streak statistics, without a clustering threshold. The table shows that, of all identified clusters that included MESH greater or equal than 6 cm, the mean hail streak is 8908 km^2. There were however only 123 clusters identified containing a MESH of this size, which is only 0.29% of the in total 41957 clusters. Most clusters, almost 96.5%, contained MESH greater or equal to 2 cm. The table suggests that damages due to hail can already occur at a hail streak of only 64 km^2, the median hail streak for hail diameters from 2 centimeters onwards. Hail sizes over 2 centimeters remain very rare as they only occur in less than 5% of the clusters.
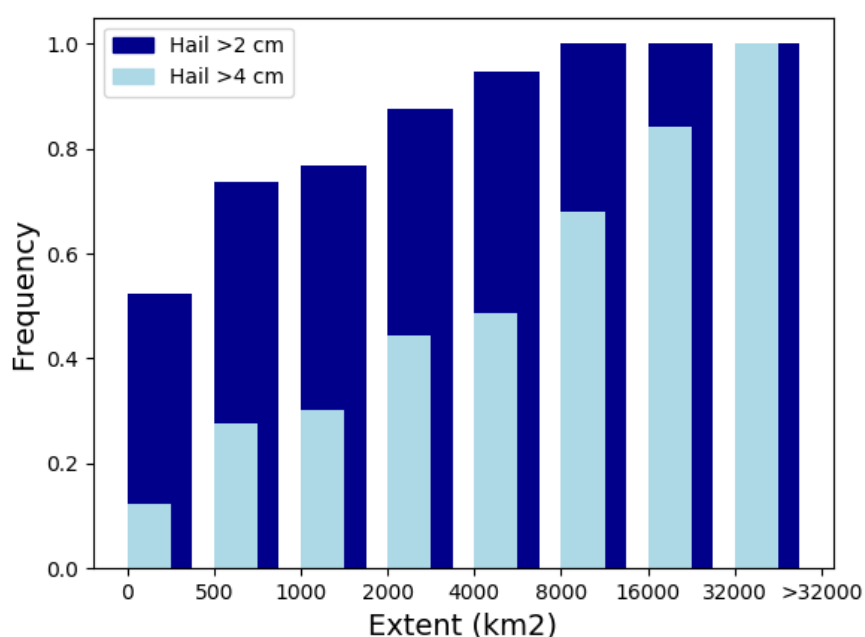
Table 5. General MESH and hail streak statistics without clustering threshold. Note: the column 'Share of total' may not count to 1 due to rounding.

MESH (cm)	Mean (km^2)	Median (km^2)	Share of total
< 1.9	12	3	0.9646
2 - 2.9	488	64	0.0191
3 - 3.9	947	133	0.0078
4 - 4.9	2856	420	0.0034
5 - 5.9	4763	757	0.0022
6 >	8908	1539	0.0029

5   Discussion

5.1   Comparison with other climatologies

In a considerable amount of countries, extensive research has been conducted on creating hail climatologies and a comparison can be made between past climatologies and the insights from more recent studies. As the literature on this topic in the Netherlands is lacking in many aspects, the climatology products of this study will also be discussed with respect to other countries and studies that focus on hail at a local or regional scale. (Botzen, et al., 2010) provide one of the few comparable sources on the annual cycle of hailfall in the Netherlands. By relating hail activity to hail damage, a trend in agricultural hail damage is also observed from May through August.

The analysis of the report-based hail dataset shows similar findings found in studies conducted on hail climatology in France (Fraile R., et al., 2003) and Germany (Junghänel, et al., 2016). In these countries, a similar pattern of hail occurrence is found with peaks from May to August. The results of (Botzen, et al., 2010) are in line with the monthly peaks in reported hail sizes found in this report. There are however countries in Europe that differ from this pattern. (Púč ik, et al., 2019) focus on report-based hail observations in the whole of Europe, and state on differences between Northern and Southern Europe. For example, large hail is reported more often in September over Corsica, February over Crete and the southern Ionian Sea, and in May over southern Greece, southern Turkey, and Cyprus. They attribute this variation to the northward migration of the polar frontal zone and the convective inhibition caused by subtropical high-pressure systems. Our study also confirms previous findings on the diurnal cycle of large hail occurrence in North-western Europe, with similar findings in France and Germany, although local variation in these countries is observed. Differences between Western and Eastern Europe are attributed to the shift of maximum diurnal heating (Púč ik, et al., 2019). As the Eastern part of Noord-Brabant and Northern part of Limburg are the warmest regions in summer, the same statement could apply to the Netherlands.

Additionally, a clear gradient in hail days is observed in the Netherlands and several reasons are mentioned in literature that could explain this variation. (Punge & Kunz, 2016) discuss the factors influencing hail frequency in Europe. They state that synoptic-scale systems are often related to severe hailstorms, including extended throughs with a centre over the West European Basin or so-called 'Spanish plumes'; well mixed and hot continental air mass moving from the Sahara or Iberian plateau to Northwest Europe. Considering the origin and general flow of these systems towards Europe, this process could explain the higher frequencies of severe hail days in the South of the Netherlands. In figure 7, we do recognize several trajectories of severe hailstorms in a similar direction. Multiple studies confirm this process to be an important factor for historic hailstorms in Belgium, France and Germany (Punge & Kunz, 2016). Another explanation could be the damping effect of the North Sea, with the large heat capacity preventing warmer temperatures and instability compared to more inland areas.

All in all, the return period estimation from the report-based hail dataset agrees with the radar-based estimates. However, the increased spatial resolution of the radar products leads to greater accuracy in determining hail-hotspots. (Fraile R., et al., 2003) make use of an extensive hailpad network to compute return periods on severe point hailfalls in France. By fitting a Gumbel distribution through the maximum annual values, a distinction in exposure to damaging hailfalls is made between administrative regions closer to the central Pyrenees and the Atlantic Ocean. Orographic factors are known to

favor hail formation, although the question arises if the limited topographic differences in the Netherlands could also lead to increased hail risk in certain regions.

Evidently, the radar-derived hail sizes show a significant relation to the observed hail sizes. The differences in the radar-derived and reported hail sizes could be explained by an insufficient lapse rate, causing the stone to melt in the time it falls to the ground. Another reason is the complication that occurs due to the horizontal movement of the stone. A storm does not only continue its course in the time the stone falls, shear and secondary convection also cause additional displacement (Salitkoff, et al., 2010). This could complicate the comparison of the radar-derived hail size at the exact location and time at which a stone is found on the ground.

The evidence that we have examined suggests that the footprint of hail streaks does relate to the size of the MESH. It is found that several Dutch hail streaks have extents up until 8000 km^2 , with almost half of them under 500 km^2 . Moreover, damaging hail diameters can occur in hail streaks with extents of only 64 km^2 . Unfortunately, no prior research could be found to strengthen these first results, confirming the importance of continued research on this topic. It should, however, be noted that, given the methodology used to compute the storm extent, relevant data outside of the Netherlands might be not included in this analysis. It is, therefore, possible that the footprints of severe hailstorms might only be captured partly, yielding footprints that might not represent the actual extent of a hailstorm. Additionally, in order to evaluate the relationship between MESH and hail streak, the smallest hail clusters were excluded. Further research is needed to investigate the relationship between MESH and hail streak extent within smaller clusters.

5.2   Climatology under climate change

As losses due to severe weather are showing an increase, it is relevant to know whether this trend could be attributed to climate change. In the last 130 years, the temperature has increased with an average of 1.0℃ with the Netherlands seeing an increase of 1.7℃. The future increases in temperature are mostly dependent on the future emissions of greenhouse gasses and the Paris agreement has the aim to restrict the worldwide temperature with 1.5℃. However, to reach this goal the emissions must decrease to zero in 2050. If the emissions are not restricted in any way, it may become 3.2 to 5.4℃ warmer globally (KNMI, 2019). The climate scenarios of the KNMI give an indication of what this means for the Netherlands based on the IPCC rapport. For the Netherlands, it is estimated that the average temperature will increase with 1.0℃ to 2.3℃ in 2050, and with 1.3℃ to 3.7℃ in 2085. Overall, the temperature will keep increasing, leading to milder winters and warmer summers.

Even though globally there is large uncertainty in the changes in frequency and intensity of hail and thunderstorms, some scenarios of hail risk in the Netherlands can be expected. Due to warmer weather, the air can hold more moisture increasing the condensation heat. This condensation heat creates strong vertical movements in clouds leading to an increase in the frequency of hail and thunder and larger hailstones. In the extremer climate scenarios, it is expected that hail occurs two times as often in 2050 compared to the period 1981-2010. This estimation is based on model calculations and the relation between moisture and vertical windspeed (KNMI, 2014).

These expected climate changes will also lead to changes in the hail climatology of the Netherlands. As stated before, the frequency of hail events and large hail sizes will increase due to higher temperatures. This indicates that the return periods of hailstones can change as well. Larger hailstones might occur more frequently, leading to larger

return periods. Another variable that is discussed in this report is the storm extent of hail events. However, it is uncertain what the effect of warmer temperatures is on the extent of a storm.

While it is uncertain how much each of the characteristics of the hail climatology will change in the future due to uncertainty temperature variation, it can be assumed that the frequency and intensity of hail will increase in the future in the Netherlands.

5.3   Event-based datasets

Accurate observational data can be limited due to an insufficient length of the time series. The use of synthetically created event-based data can help to overcome the issue. By using the statistical parameters of the original data, synthetic hazard events can be modelled corresponding to historical physical and environmental characteristics of a hazard. An example of such an application is given in the study of Filipova et al., (2019) for flood estimation. Here a traditional flood frequency analysis and an event-based model is extended with a stochastic model by considering different combinations of initial conditions such as rainfall and snowmelt, from which a distribution of flood peaks can be constructed. By doing so, the results for any return period can be derived, considering the probability of a range of possible initial conditions. It was observed that the approach gives good fits to observed POT approaches. Particularly for compensations schemes (or insurance) related to hail events, it is important to also move towards event-based hail datasets, but these do not exist publicly yet for the Netherlands.

5.4   Now-casting

The radar data that is used in this study to determine the hail climatology of the Netherlands, can also be used for different purposes. An example of a valuable purpose can be the use of the radar data for now-casting hail events. Now-casting is the detailed description of the current weather along with forecasts obtained by extrapolation for a period of 0 to 6 hours ahead (World Meteorological Organization, 2019). In this short time range, it is possible to forecast storms quite accurately. Although the results of this study show that the MESH is not always in agreement with eye-witness observations, it can give a good indication of the severity of the hail. Additionally, the lack of agreement can also be due to a mismatch in time and place of the radar-based and eye-witness observations and not due to the inaccuracy of the radar-based data. Figure 15 shows an example of now-casting development at the KNMI. It shows the radar reflectivity together with the expected path of the event. The development of such a tool may be very useful for taking short-term actions to protect objects from hail, such as cars, windows and solar panels. Another promising line of research is the real-time extraction of information from social media. This method is already applied to the detection of floods or earthquakes (de Bruijn, et al., 2019). Adapting this technique and combining it with current nowcasting systems could provide real-time information from both radar-derived and eyewitness-based observations, potentially reducing the warning-area and improving impact estimates.
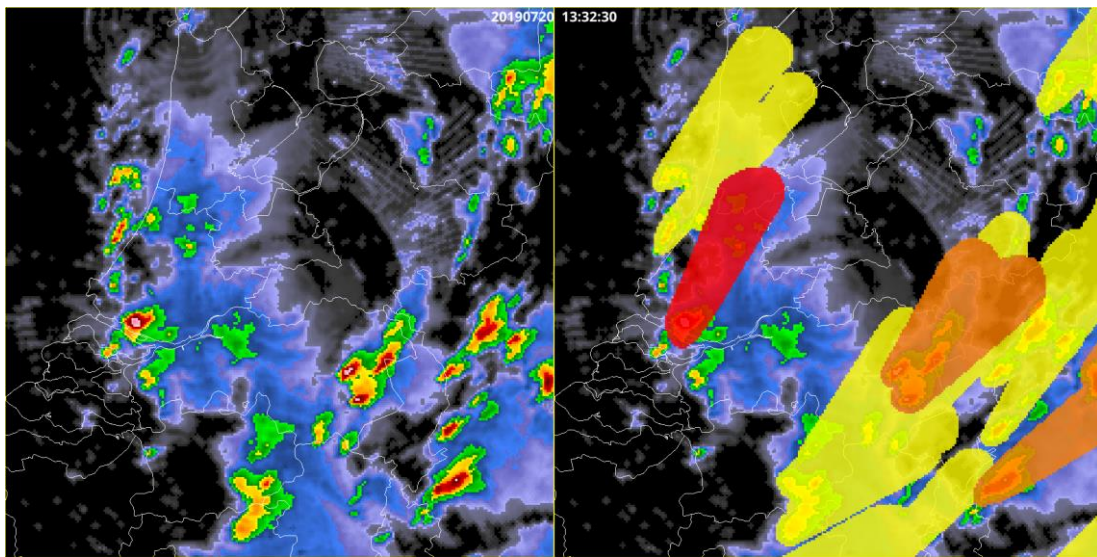
Figure 14. Now-casting of the severity and direction of intense reflectivity using radar.

6   Conclusion

Information from written documents and radar-derived products were evaluated to extend the current knowledge about hail characteristics in the Netherlands. Several important contributions to a hail climatology in the Netherlands are made:

- It is found that most hail events occur in the convective season (May-August) with peak hours between 14:00 and 19:00 local time. In total, 81% of all hail events above 2 cm and 95% of all events with hail larger than 4 cm are reported in this season.

- The spatial distribution of radar-derived maximum diameter values and the number of severe hail days imply a division in hail risk between the North-western and South-eastern regions of the Netherlands. The highest average MESH values are observed in Noord-Brabant and Limburg with values of 4.1 and 4.3 cm, respectively, and lowest in Friesland and Noord-Holland with values of 3.3 and 3.2, respectively.

- The return period estimation from report-based hail sizes indicate an occurrence of 1 in 100 years in the case of diameter equal or larger than 11 cm, 1 in 50 years of diameter equal or larger than 9 cm and 1 in 10 years of diameter equal or larger than 7 cm for the Netherlands. By dividing the country into geographically representative regions (NUTS1), a distinction can be made between them. The Northern NUTS region yields lower overall exceedance probabilities than the Southern NUTS region, in line with the spatial distribution observed in written records and the number of hail days.

- By clustering hail events into induvial storms, an increasing trend in MESH values was observed with increasing hailstorm extent, though large hailstone sizes can also occur in small hail streaks.

- Literature from other climatologies provides insight into the differences found in regions in the Netherlands. A possible explanation is given by a combination of large-scale flow conditions and the dampening effect of the North Sea.

Although this research has uncovered several important factors that influence hail risks in the Netherlands, the effects of climate change and increasing exposure point to the compelling need for further research. Quantitative research on climate variation and its effect on hail sizes and frequencies is necessary to prepare for different climate scenarios. Furthermore, the development of nowcasting systems, and the potential integration with information from social media, could provide real-time information on hail. If successful, timely measures can be taken to reduce the potential impacts on a local scale. Lastly, by continually updating the climatology, a more robust analysis can be made. Therefore, it is recommended to extend this research in the coming years and include new findings in the climatology.

7   References

Allen, J. T. (2007). Atmospheric hazards: Hail potential heating up. *Nature Climate Change*, 474.

Bezak, N., Brilly, M., & Šraj, M. (2014). Comparison between the peaks-over-threshold method and the annual maximum method for flood frequency analysi. *Hydrological Sciences Journal*, 959 - 977.

Botzen, W., Bouwer, L., & van den Bergh, J. (2010). Climate change and hailstorm damage: Empirical evidence and implications for agriculture and insuranc. *Resource and Energy Economics*, 341-362.

Brimelow, J. C., Burrows, W. R., & Hanesiak, J. M. (2017). The changing hail threat over North America in response to anthropogenic climate change. *Nature Climate Change*, 516.

Bunkers, M. J., & Smith, P. L. (2013). Comments on ''An Objective High-Resolution Hail Climatology of the Contiguous United States''. *American Meteorological Society*.

Burcea, S. (2016). Hail Climatology and Trends in Romania: 1961–2014 . *Monthly Weahter Review*.

Cintineo, J. L., Smith, T. M., & Lakshmanan, V. (2012). An Objective High-Resolution Hail Climatology of the Contiguous United States . *Weather and Forecasting*.

de Bruijn, J., de Moel, H., Jongman, B., de Ruiter, M., Wagemaker, J., & Aerts, J. (2019). A global database of historic and real-time flood events based on social media. *Scientific Data*.

Dennis, E. J., & Kumjian, M. R. (2017). The impact of vertical wind shear on hail growth in simulated supercells. *Journal of the Atmospheric Sciences*, 641-663.

Dubin, R. (2009). *The Sage handbook of spatial analysis.* SAGE publications Ltd.

EIT Climate-KIC. (2018). *1 Million near-zero eneger/carbon neutral homes.* Budapest: European Institute of Innovation & Technology.

Filipova, V., Lawrence, D., & Skaugen, T. (2019). A stochastic event-based approach for flood estimation in catchments with mixed rainfall and snow melt flood regime. *Natural Hazard and Earth System Sciences*.

Fraile, R., Berthet, C., Dessens, J., & Sánchez, J. L. (2003). Return periods of severe hailfalls computed from hailpad data. *Atmospheric Research*, 189-202.

Groenemeijer, P., & van Delden, A. (2005). Sounding-derived parameters associated with large hail and tornadoes in the Netherlands. *Atmospheric research*, 473 - 487.

Holleman, I. (2001). *Hail detection using single-polarization radar.* KNMI.

Ilotoviz, E., Khain, A. P., Benmoshe, N., Phillips, V. T., & Ryzhkov, A. V. (2016). Effect of aerosols on freezing drops, hail, and precipitation in a midlatitude storm. *Journal of the Atmospheric Sciences*, 109-144.

Junghänel, T., Brendel, C., Winterrath, T., & Walter, A. (2016). Towards a radar- and observation-based hail climatology for Germany. *Meteoreologische Zeitschirft*, 435-445.

KNMI. (2014). *KNMI Klimaatscenario's voor Nederland '14.* De Bilt: Ministerie van Infrastructuur en Milieu.

KNMI. (2019, December 11). *Klimaatverandering*. Opgehaald van KNMI: https://www.knmi.nl/kennis-en-datacentrum/uitleg/klimaatverandering

Mahoney, K., Alexander, M. A., Thompson, G., Barsugli, J. J., & Scott, J. D. (2012). Changes in hail and flood risk in high-resolution simulations over Colorado's mountains. *Nature Climate Change*, 125.

Mohr, S., & Kunz, M. (2013). Recent trends and variabilities of convective parameters relevant for hail events in Germany and Europe. *Atmospheric Research*, 211-228.

Munich RE. (2019, December 2). *Risks; Natural Disaster Risks; Thunderstorm, hail and tornadoes.* Opgehaald van Munich RE: https://www.munichre.com/en/risks/natural-disasters-losses-are-trending-upwards/thunderstorms-hail-and-tornados.html

Musayev, S., Burgess, E., & Mellor, J. (2018). A global performance assessment of rainwater harvesting under climate change. *Resources, Conservation & Recycling*, 62-70.

Ortega, K., Smith, T., Manross, K., Scharfenberg, K. W., Kolodziej, A., & Gourley, J. (2009). The Severe Hazards Analysis and Verfication Experiment. *Bulletin of the American Meteorological Society*, 1519-1530.

Púčik, T., Castellano, C., Groenemeijer, P., & Kühne, T. (2019). Large Hail Incidence and Its Economic and Societal Impacts across Europe. *Montly Weather Review*, 3901 - 3916.

Punge, H., & Kunz, M. (2016). Hail observations and hailstorm characteristics in Europe: A review. *Atmospheric research*, 159-184.

Riemann-Campe, K., Fraedrich, K., & Lunkeit, F. (2009). Global climatology of convective available potential energy (CAPE) and convective inhibition (CIN) in ERA-40 reanalysis. *Atmospheric research*, 534-545.

Salitkoff, E., Tuovinen, J., Kotro, J., Kuitunen, T., & Hohti, H. (2010). A Climatological Comparison of Radar and Ground Observation of Hail in Finland. *Applied Meteorology and Climatology*, 101-114.

Sanchez, J. L., Merino, A., Melcón, P., García-Ortega, E., Fernández-González, S., Berthet, C., & Dessens, J. (2017). Are meteorological conditions favoring hail precipitation change in Southern Europe? Analysis of the period 1948–2015. *Atmospheric research*, 198.

Teule, T., Appeldoorn, M., Bosman, P., Sprenger, D., Kloek, G., Vermunt, R., . . . De Moel, H. (2019). *The vulnerability of solar panels to hail.* Amsterdam: Institute of Envriromental Studies.

Thom, H. C. (1957). The frequency of hail occurrence. *Archiv für Meteorologie, Geophysik und Bioklimatologie,*, 185-194.

Verbond Van Verzekeraars. (2017). *Hoofd Boven Water; verzekeren van schade in een veranderend klimaat.* Verbond Van Verzekeraars.

Vujović, D. P. (2015). Evaluation of the stability indices of the thunderstorm forecasting in the region of Belgrade, Serbia. *Atmospheric Research*, 143-152.

Waldvogel, A., Schmid, W., & Federer, B. (1978). The kinetic energy of hailfalls. Part I: hailstone spectra. *Atmospheric Physics*, 515 - 520.

Witt, A., Eilts, M. D., Stumpf, G. J., Jonhson, J., Dewayne Mitchell, E., & Thomas, K. W. (1998). An Enhanced Hail Detection Algorithm for the WSR-88D. *Weather and Forecasting*, 286-303.

World Meteorological Organization. (2019, December 6). *Now-casting*. Opgehaald van World Meteorological Organization: https://www.wmo.int/pages/prog/amp/pwsp/Nowcasting.htm

Zou, T., Zhang, Q., Li, W., & Li, J. (2018). Responses of hail and storm days to climate change in the Tibetan Plateau. *Geophysical Research Letters*, 4485-4493.